


Carbonization of Silicon Nanoparticles via Ablation Induced by Femtosecond Laser Pulses in Hexane

Xi Yu¹  · Shusaku Terakawa¹ · Shunsuke Hayashi¹ · Toru Asaka¹ · Fumihito Itoigawa¹ · Shingo Ono¹ · Jun Takayanagi²

Received: 17 February 2017 / Accepted: 10 May 2017 / Published online: 25 May 2017
© King Fahd University of Petroleum & Minerals 2017

Abstract Silicon carbide (SiC) has been widely used in various technological applications, including power devices, light-receiving devices, and light-emitting devices. Several methods for fabricating SiC particles with nanometer dimensions have been reported, including carbo-thermal reduction of silica, chemical vapor deposition, laser pyrolysis, and microwave irradiation. To develop a new and simple method for fabricating SiC nanoparticles, we investigated the possibility of using femtosecond-laser ablation. In this paper, we report the formation of SiC nanoparticles by femtosecond-laser ablation on silicon immersed in hexane. By using a high-peak-power laser that can achieve extremely high temperatures and pressures on the silicon surface, SiC nanoparticles were successfully fabricated via ablation in hexane. In our experiments, femtosecond pulses from a Yb-fiber laser were used to irradiate to silicon single crystal. The laser was focused onto a spot on the silicon surface. After ablation, we evaluated the particles on the target substrate and particles in the irradiated hexane. Scanning electron microscopy revealed that the particles range in size from 100 to 400 nm. X-ray diffraction analysis indicated that the nanoparticles might be SiC. The characteristic X-ray photoelectron spectroscopy peaks of nanoparticles were Si-2*p* (100.1 eV) and C-1*s* (282.9 eV), which are identical to the characteristic peaks of SiC (John et al. in Handbook of X-ray photoelectron spectroscopy, Physical Electronics, Eden Prairie, 1995;

Hijikata et al. in Appl Surf Sci 184:161–166, 2001; Shen et al. in Chem Phys Lett 375:177–184, 2003). We also used transmission electron microscopy and electron energy-loss spectroscopy to evaluate particles from the irradiated hexane. Such a simple method of fabricating SiC nanoparticles by femtosecond-laser ablation may open new possibilities in the development of growth techniques for SiC.

Keywords Silicon carbide · Nanoparticles · Femtosecond laser · Under-liquid processing · Laser ablation

1 Introduction

Silicon carbide (SiC) has attracted the attention of researchers because of its excellent mechanical and electrical properties [4,5]. For example, its hardness ranks third behind those of diamond and cubic boron nitride (c-BN). Its thermal stability and abrasion resistance are also excellent. Because of these excellent mechanical properties, SiC is used as a structural ceramic in components of gas turbines or automobiles [4,6]. SiC is also a semiconductor with numbers favorable electrical properties, such as a wide bandgap, high thermal conductivity, and a high saturated electron drift velocity; as such, SiC has found applications in power devices, UV-light photodiodes, and UV-light emitters. High-temperature applications are also expected [5,7,8]. The demand for SiC nanoparticles (~100 nm) as a ceramic raw material for UV-light photodiodes and UV-light emitters has been increasing [9].

Various chemical vapor deposition (CVD) methods, including thermal CVD, RF plasma, arc-plasma, and laser CVD, have been developed as the main methods for fabricating SiC nanoparticles [10–13]. However, these methods require a vacuum pumping system and a collection pro-

✉ Shingo Ono
ono.shingo@nitech.ac.jp

¹ Nagoya Institute of Technology, Nagoya 4668555, Japan

² Aisin Seiki Co., Ltd., Kariya 4488650, Japan

cessing system. Because of these processing conditions, processes become longer and the devices become complex. New methods are demanded.

In this research, we aimed at developing a relatively simple method of fabricating SiC nanoparticles. We used a femtosecond laser to irradiate the Si substrate in hexane. We then characterized the particles on surface of target substrate, as well as particles in the irradiated hexane. The results suggest that SiC nanoparticles are fabricated by this new method.

2 Experimental Methods

Liquid-phase laser ablation is one method available for synthesizing nanoparticles [14–17]. In recent years, attention has been focused on using a femtosecond laser, which can the ability to irradiate with extremely high peaking power to provide high-temperature, high-pressure conditions [18]. When a pulsed laser beam is focused on a target in liquid, a high-temperature, high-pressure region will be generated in the focused area and the target material will be ablated into particles such as atoms, molecules, ions, or radicals. The ablated particles can also react with pyrolyzed solvent to form new particles.

In this research, we used a femtosecond laser to irradiate a Si substrate immersed in hexane. As shown in Fig. 1, at the interface, the laser ablation results in the formation of Si particles react with carbon species pyrolyzed from hexane (C_6H_{14}) to form SiC nanoparticles. In addition, the hexane provides oxygen-free conditions, inhibiting the formation of silicon oxide.

Figure 2 is a schematic of the experimental setup. A Si substrate was immersed in a quartz cell filled with hexane. The substrate was then irradiated using femtosecond laser pulses with a wavelength of 1045 nm, a pulse width of 700 fs, and a repetition rate of 100 kHz. The laser beam was focused on the substrate using an objective lens with a fluence of $31.4 J/cm^2$.

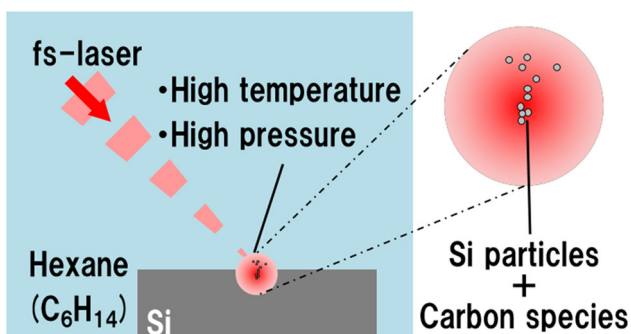


Fig. 1 The ablated Si particles are combined with carbon species to form SiC at the interface

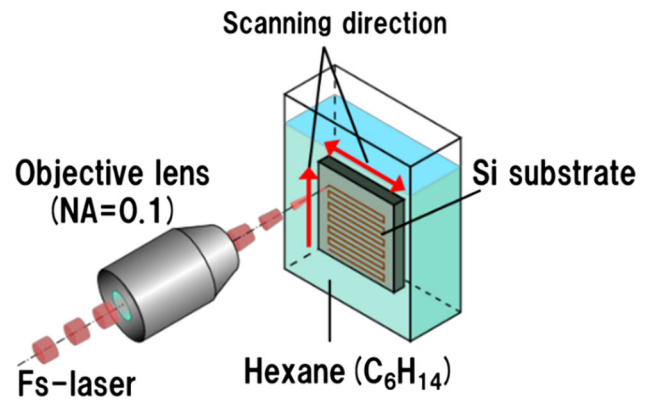


Fig. 2 Schematic of the experimental setup

The Si substrate was adhered to a two-axis motorized stage, which enabled the Si substrate to be scanned at a stable speed of $100 \mu m/s$. The scanning distance was 580 mm over 97 min.

The irradiated Si substrate was prepared as a Si single crystal with (1-0-0) plane orientation. The irradiated side was polished. The thickness of the Si substrate was $505 \mu m$. The purity of the hexane was 96%. The chemical formula is $CH_3(CH_2)_4CH_3$, and its standard is JIS-K-8848.

After the irradiation, we evaluated the particles on the target substrate, by using scanning electron microscopy (SEM), X-ray photoelectron spectroscopy (XPS), and X-ray diffraction (XRD) and evaluated the particles in the irradiated hexane using transmission electron microscopy (TEM) in conjunction with electron energy-loss spectroscopy (EELS).

3 Results and Discussions

3.1 SEM Analysis

Figure 3a, b shows SEM micrographs of the Si substrate after laser ablation. As shown in Fig. 3a, spherical nanoparticles were deposited in an approximately $1.3\text{-}\mu m$ -thick layer onto the substrate. Figure 3b shows that the particle size was relatively large ($> 100 \text{ nm}$). We estimate that ablated atoms and clusters tend to aggregate into much larger particles via thermal effects during or after the laser pulse [16]. We measured the particle size and its distribution for 200 particles from the SEM image; the results, which are shown in Fig. 3c, suggest that, at the fluence of $31.4 J/cm^2$, the particle size is distributed at a center of 230 nm.

3.2 XRD Analysis

The crystal structure of the nanoparticles on the Si substrate was analyzed by powder XRD. In the diffraction pattern shown in Fig. 4, peaks attributed to β -SiC are observed

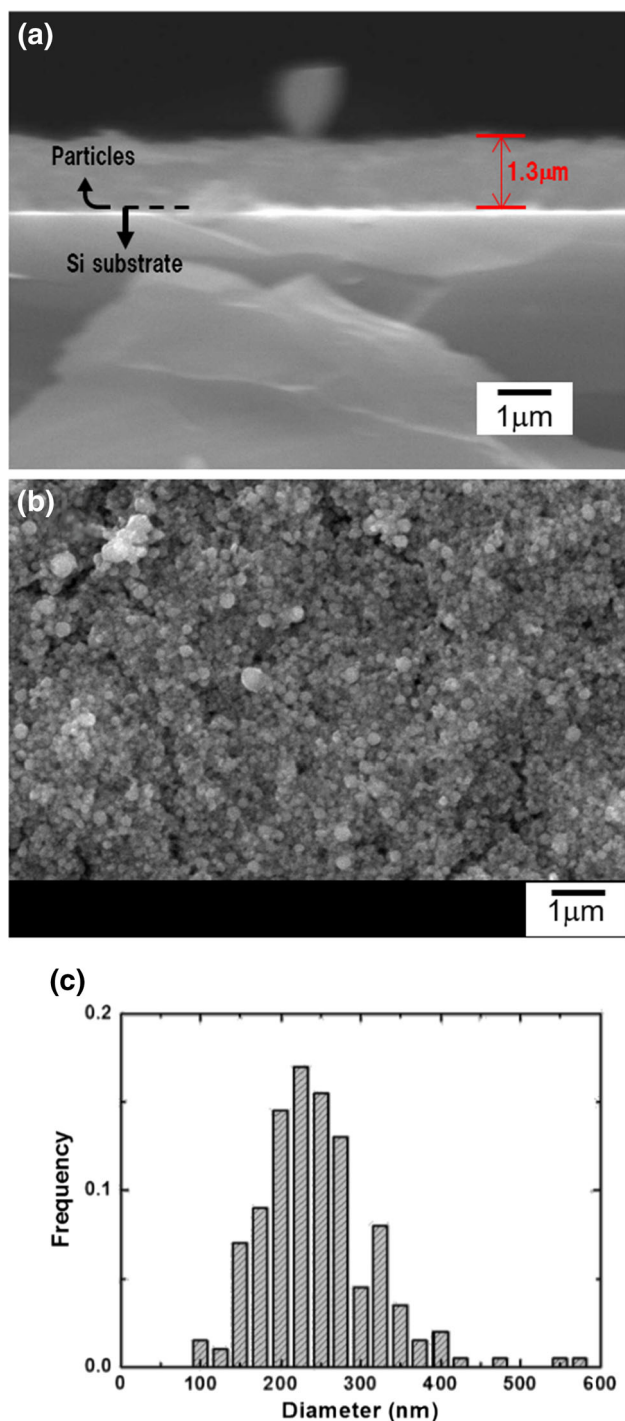


Fig. 3 **a** Sectional view of the Si substrate; **b** SEM image of particles deposited onto the Si substrate; **c** particle size distribution measured from the SEM image in **b**

at 35.62° and 59.94° (ICDD-PDF #01-074-2307). Peaks attributed to SiO_2 and SiO are not observed; however, these phases could be an amorphous and the peaks may be obscured by the background.

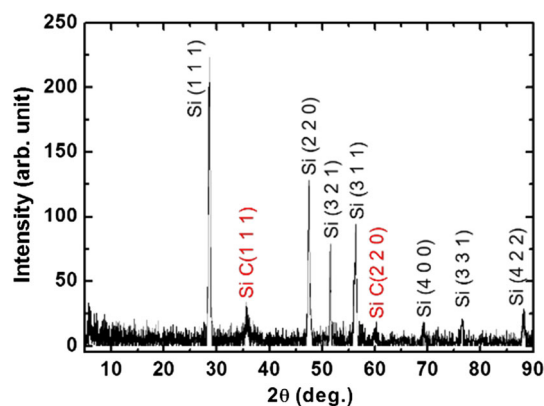


Fig. 4 XRD pattern of particles deposited onto the Si substrate

3.3 XPS Analysis

The chemical bonds of nanoparticles were analyzed by XPS. The ablated sample was treated by Ar etching for 5 min to remove surface contamination. The survey spectrum indicated that nanoparticles are composed of only Si, C, and O. Figure 5 shows the narrow-scan spectra of Si-2*p*, C-1*s*, and O-1*s*. Peak fitting was performed using mixed Gaussian/Lorentzian function, and the background was treated using the Shirley method [19]. Table 1 shows the distribution of the synthesized materials calculated from the fitting results.

In the Si-2*p* spectrum (Fig. 5a), a peak attributed to Si–C bonds with a binding energy of 100.6 eV was observed, indicating the formation of SiC. In addition, other peaks were observed at 99.2, 101.7, and 102.8 eV, which were identified as Si–Si, Si–O, and Si–O₂ bonds [1, 2, 20]. These results indicate the formation of Si particles unreacted with carbon in addition to an oxidized phase. Small peaks from different electronic spins are also observed, with a separation of 0.61 eV and an area ratio of 2:1.

The C-1*s* spectrum (Fig. 5b) shows two peaks with binding energies of 284.6 and 283.1 eV, which are attributed to C–C and C–Si bonds, respectively [1, 20, 21].

In the O-1*s* spectrum (Fig. 5c), two peaks attributed to O₂–Si and O–Si bonds are observed at 532.7 and 532.1 eV, respectively [2, 20]. Despite the use of hexane, which does not contain oxygen, an oxygen peak was detected. Because silicon is easily oxidized in the atmosphere, the Si particles may have already been oxidized before the laser ablation.

For comparison, we used XPS to analyze an unprocessed Si substrate whose surface had been subjected to Ar etching for 1 min. The results are shown in Fig. 6. Peaks are observed at 99.3, 101.8, and 102.4 eV, which are identified as Si–Si, Si–O, and Si–O₂ bonds, respectively [1, 2, 20]; however, the Si–C peak did not appear (Fig. 6a). In addition, the narrow-scan C-1*s* spectra show only background noise, which means no SiC was present on the Si substrate before processing. The

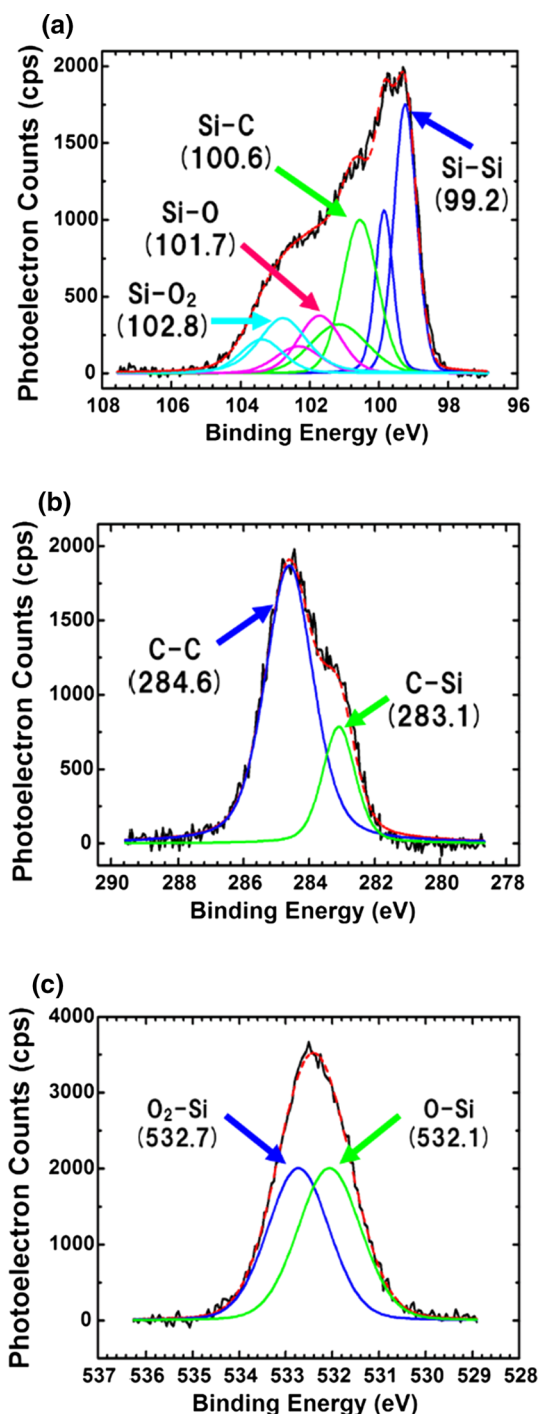


Fig. 5 XPS narrow-scan spectra of particles deposited onto the Si substrate: **a** Si-2*p*, **b** C-1*s*, and **c** O-1*s*

spectrum in Fig. 6b shows peaks at 532.7 and 531.7 eV, which are attributed to O₂-Si and O-Si bonds, respectively [2,20].

3.4 TEM and EELS Analysis

Figure 7 shows the TEM particle analysis results and the EELS elemental mapping images of Si and C. The particles

Table 1 The composition ratio of synthesized nanoparticles, as determined by XPS

Formula	Ratio (%)
C	32
SiC	20
SiO ₂	18
SiO	17
Si	13

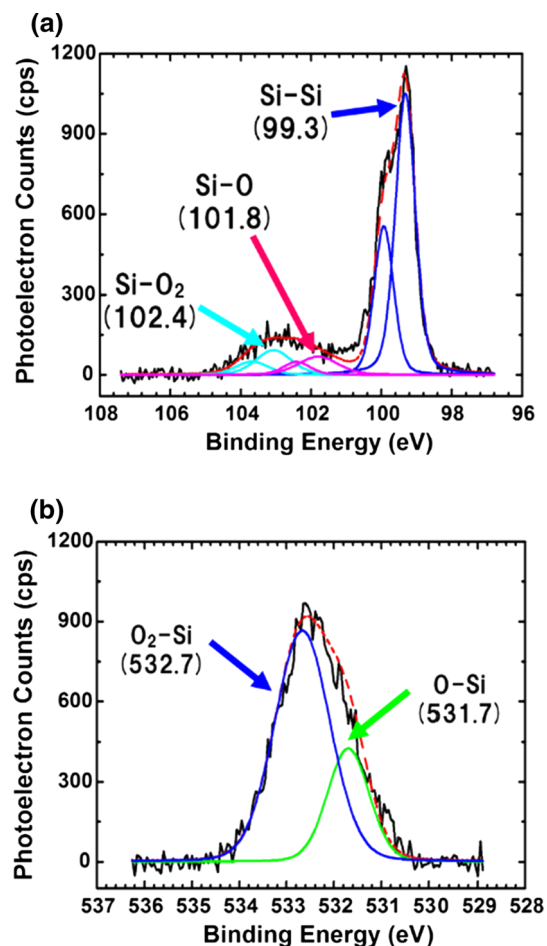


Fig. 6 XPS narrow-scan spectra of an unprocessed Si substrate **a** Si-2*p* and **b** O-1*s*

were collected by ultrasonic cleaning of the Si substrate in ethanol, and then dropped on to a TEM microgrid. In the TEM image in Fig. 7a, we focused on two particles: one smaller than 100 nm (particle A) and one larger than 100 nm (particle B). A comparison of these two particles revealed differences in their crystallinity. Particle A is a single crystal; however, different orientations are observed from particle B, indicating that it is polycrystalline.

The elemental mapping images of Si (Fig. 7b) and C (Fig. 7c) reveal a difference in the distribution of carbon. Whereas carbon is distributed homogeneously in particle A, it is only detected in the area near the surface of particle B.

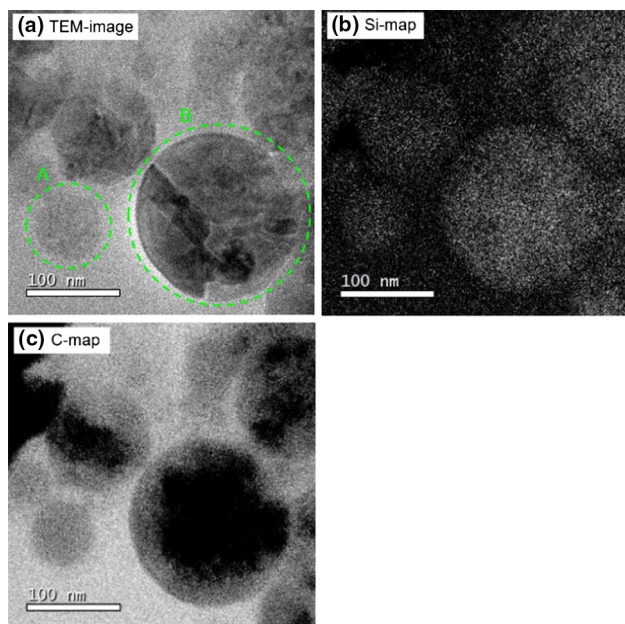


Fig. 7 a TEM image of synthesized particles and EELS mapping images of b Si and c C

These results suggest that large particles are not completely carbonized to SiC and that the inner area of such particles remains unreacted Si. On the basis of these results, we assume that, in the case of particles larger than 100 nm, insufficient thermal energy to form SiC reaches the inner area of the particle, thus resulting in the inner area remaining unreacted Si.

4 Conclusions

We successfully synthesized SiC nanoparticles by femtosecond-laser ablation of a Si substrate in hexane. Although the size distribution measured from the SEM images indicated the formation of sub-micrometer-sized particles, nanoparticles smaller than 100 nm were observed in the corresponding TEM images. According to the XPS and XRD results, the obtained materials consisted of SiC, Si, SiO₂, and SiO. The EELS results indicated that particles larger than 100 nm were not completely carbonized, but their extent of carbonization might be improved through adjustment of the laser parameters. In the case of particles smaller than 100 nm, Si and C were distributed homogeneously, indicating the formation of SiC. These results demonstrate the potential of this method as a new simple single-step approach to fabricating SiC nanoparticles.

Acknowledgements This work was partly supported by the Nanotechnology Platform Program (Molecule and Material Synthesis) of

the Ministry of Education, Culture, sports, Science and Technology (MEXT), Japan. This work was supported by a Grant-in-Aid for Scientific Research (C) (Grant Number 16K04961) from the Japan Society for the Promotion of Sciences (JSPS).

References

1. John, M.; William, F.S.; Peter, E.S.; Kenneth, D.B.: Handbook of X-Ray Photoelectron Spectroscopy, pp. 40–45, 56–57, 216, 230–231, 238. Physical Electronics, Eden Prairie (1995)
2. Hijikata, Y.; Yaguchi, H.; Yoshikawa, M.; Yoshida, S.: Composition analysis of SiO₂/SiC interfaces by electron spectroscopic measurements using slope-shaped oxide films. *Appl. Surf. Sci.* **184**, 161–166 (2001)
3. Shen, G.; Chen, D.; Tang, K.; Qian, Y.; Zhang, S.: Silicon carbide hollow nanospheres, nanowires and coaxial nanowires. *Chem. Phys. Lett.* **375**, 177–184 (2003)
4. Reau, A.; Guizard, B.; Canel, J.; Galy, J.; Tenegal, F.: Silicon carbide nanopowders: the parametric study of synthesis by laser pyrolysis. *J. Am. Ceram. Soc.* **95**, 153–158 (2012)
5. Weitze, C.E.; Palmour, J.W.; Carter, C.H.; Moore, K.; Nordquist, K.K.; Allen, S.; Thero, C.; Bhatnagar, M.: Silicon carbide high-power devices. *IEEE Trans. Electron Devices* **43**, 1732–1741 (1996)
6. Larpiattaworn, S.; Ngerchuklin, P.; Khongwong, W.; Pankurdee, N.; Wada, S.: The influence of reaction parameters on the free Si and C contents in the synthesis of nano-sized SiC. *Ceram. Int.* **32**, 899 (2006)
7. Chen, X.; Zhu, H.; Cai, J.; Wu, Z.: High-performance 4H-SiC-based ultraviolet pin photodetector. *J. Appl. Phys.* **102**, 024505 (2007)
8. Zakharko, Y.; Botsoa, J.; Alekseev, S.; Lysenko, V.; Bluet, J.M.; Marty, O.; Skryshevsky, V.A.; Guillot, G.: Influence of the interfacial chemical environment on the luminescence of 3C-SiC nanoparticles. *J. Appl. Phys.* **107**, 013503 (2010)
9. Yu, I.K.; Rhee, J.H.; Cho, S.; Yoon, H.K.: Design and installation of DC plasma reactor for SiC nanoparticle production. *J. Nucl. Mater.* **386–388**, 631–633 (2009)
10. Kavecky, S.; Janekova, B.; Madejova, J.; Sajgalik, P.: Silicon carbide powder synthesis by chemical vapour deposition from silane/acetylene reaction system. *J. Eur. Ceram. Soc.* **20**, 1939–1946 (2000)
11. Sachdev, H.; Scheid, P.: Formation of silicon carbide and silicon carbonitride by RF-plasma CVD. *Diam. Relat. Mater.* **10**, 1160 (2001)
12. Kijima, K.; Noguchi, H.; Konishi, M.: Sintering of ultrafine SiC powders prepared by plasma CVD. *J. Mater. Sci.* **24**, 2929–2933 (1989)
13. Cauchetier, M.; Croix, O.; Luce, M.; Michon, M.; Paris, J.; Tistchenko, S.: Laser synthesis of ultrafine powders. *Ceram. Int.* **13**, 13–17 (1987)
14. Hu, A.; Sanderson, J.; Zhou, Y.; Duley, W.W.: Formation of diamond-like carbon by fs laser irradiation of organic liquids. *Diam. Relat. Mater.* **18**, 999–1001 (2009)
15. Compagnini, G.; Scalisi, A.A.; Puglisi, O.: Production of gold nanoparticles by laser ablation in liquid alkanes. *J. Appl. Phys.* **94**, 7874 (2003)
16. Kabashin, A.V.; Meunier, M.: Synthesis of colloidal nanoparticles during femtosecond laser ablation of gold in water. *J. Appl. Phys.* **94**, 7941 (2003)
17. Simakin, A.V.; Voronov, V.V.; Kirichenko, N.A.; Shafeev, G.A.: Nanoparticles produced by laser ablation of solids in liquid environment. *Appl. Phys. A Mater. Sci. Process.* **79**, 1127–1132 (2004)



18. Juodkazis, S.; Nishimura, K.; Tanaka, S.; Misawa, H.; Gamaly, E.G.; Luther-Davies, B.; Hallo, L.; Nicolai, P.; Tikhonchuk, V.T.: Laser-induced microexplosion confined in the bulk of a sapphire crystal: evidence of multimegabar pressures. *Phys. Rev. Lett.* **96**, 161101 (2006)
19. Tougaard, S.; Jansson, C.: Background correction in XPS: comparison of validity of different methods. *Surf. Interface Anal.* **19**, 171–174 (1992)
20. Nguyen, T.P.; Lefrant, S.: XPS study of SiO thin films and SiO-metal interfaces. *J. Phys. Condens. Matter* **1**, 5197–5204 (1989)
21. Lan, J.; Yang, Y.; Li, X.: Microstructure and microhardness of SiC nanoparticles reinforced magnesium composites fabricated by ultrasonic method. *Mater. Sci. Eng. A* **386**, 284–290 (2004)

